Fracture Mechanics of Concrete and Concrete Structures - High Performance, Fiber Reinforced Concrete, Special Loadings and Structural Applications- B. H. Oh, et al. (eds)

Durability performance of UFC sakata-mira footbridge under sea environment

Y. Tanaka & H. Musha
Taisei Corporation, Tokyo, Japan

S. Tanaka & M. Ishida
Taiheiyo Cement Corporation, Tokyo, Japan

ABSTRACT: Sakata-Mirai Footbridge has been completed for the first time in Japan using ultra high performance fiber reinforced concrete, brand name Ductal® in October 2002. The location of this footbridge is about 3.4 km from the Japan Sea coastline therefore this footbridge has been exposed to severe corrosive environment in winter. In this paper the diffusion coefficient of chloride ions and the mechanical properties were investigated form the field observation. Also the pore size distribution investigation applying the mercury intrusion porosimetry apparatus were carried out in the laboratory. The advantage of the life cycle cost of UHPFRC structures in chloride ions attack is discussed.

1 INTRODUCTION

The brand name Ductal® is one of the most applied Ultra High Performance Fiber Reinforced Concrete (abbreviated to UFC) materials for actual structures such as bridges, buildings, tunnel lining and so on in the world. Recent ten years, around twenty structures were constructed applying Ductal® in Japan. As Ductal® is new generation concrete material possessing high strength, high ductility, high fluidity and high durability, it is possible to drastically reduce the dead weight of the bridges compared to those made of ordinary concrete and this can reduce the total construction cost including the foundation cost especially in earthquake countries like Japan. Furthermore, the maintenance cost can be saved due to its high durability performance.

In 2002, a 50 m span "Sakata-Mirai Footbridge" (Tanaka et al. 2002) has been constructed in Sakata City applying Ductal® for the first time in Japan as shown in Photograph 1. Based on this achievement and laboratory test data, "Recommendations for Design and Construction of Ultra High Strength Fiber Reinforced Concrete Structures, -Draft" (JSCE 2004) was published in 2004 by Japan Society of Civil Engineers. After the publication, the design and construction records of footbridges, highway bridges, railway bridges and architectural structures made of UFC have been increasing for recent five years in Japan.

This footbridge is located in Sakata City facing to the Japan Sea and the site location is about 3.4 km from the Japan Sea coastline. The footbridge has been attacked by severe corrosive winds in winter. In order to prove that the footbridge would not need any maintenance, authors have been investigating the durability behavior and its mechanical strength performance of the footbridge through monitoring the test specimens exposed inside the box girder of the footbridge.


Photograph 1. Completion of Sakata-Mirai Footbridge.

2 CONSTRUCTION OF FOOTBRIDGE

2.1 *Site location*

The footbridge is located in Sakata City, Yamagata prefecture facing to the Japan Sea. The location map of this footbridge is shown in Figure 1. The west coastline in Japan usually has severe west or south

Figure 1. Site location map of footbridge.

Table 1. Composition of Ductal®.

unit	mixed ingrediant (cement, silica fume, quartz, etc)	water	fiber	super plastcizer	W/C
kg/m^3	2254	180	157	24	22

west winds and snowy storm in winter. Although the site location is 3.4 km far from the coastline, the seasonal winter storms induce the chloride attack on the footbridge.

2.2 *Material performance applied for footbridge*

The formulation of Ductal® applied for Sakata-Mirai Footbridge is shown in Table 1. The major principles are as follows; 1) minimum of defects such as micro-cracks and pore spaces by extremely low water/cement ratio (=22%), 2) enhancement of compacted density by optimization of the granular mixture, 3) enhancement of the microstructure by heat treatment, and 4) enhancement of ductility by incorporating steel fiber. The self-leveling performance is achieved that a flow value (JIS-R-5202.11) is around 240-260 mm for the material temperature of 20~25°C even for including the steel fiber (0.2 mm in diameter, 15 mm in length) by 157 kg/m^3 (2% in vol.) in the matrix. Therefore it is possible to cast it into the very thin shell mold or into the complicated shaped mold. The segregation or sinking of steel fiber from the matrix does not occur because of the viscousity of the paste. However it is noted that the orientation of the steel fiber should be controlled to distribute in all directions when casting.

The mixing plant for the fabrication of pre-cast segments was an ordinary pan type mixer. For the

mechanical quality management of the material, 6 test cylindrical specimens with the size of ϕ10x20 cm for compressive strength and 3 test specimens with the size of 10x10x40 cm for flexural strength were sampled for each pre-cast segments. All

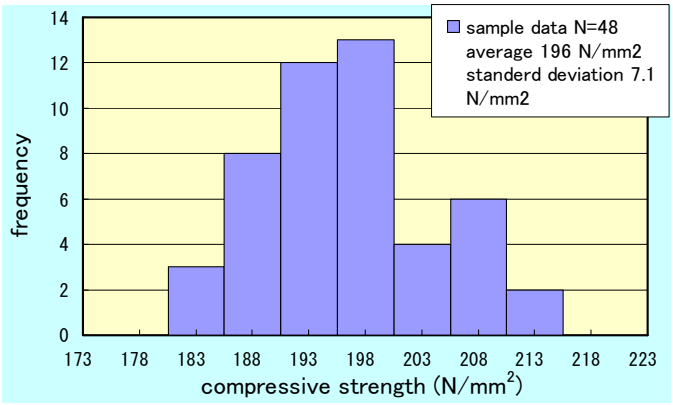

Figure 2. Compressive strength frequency.

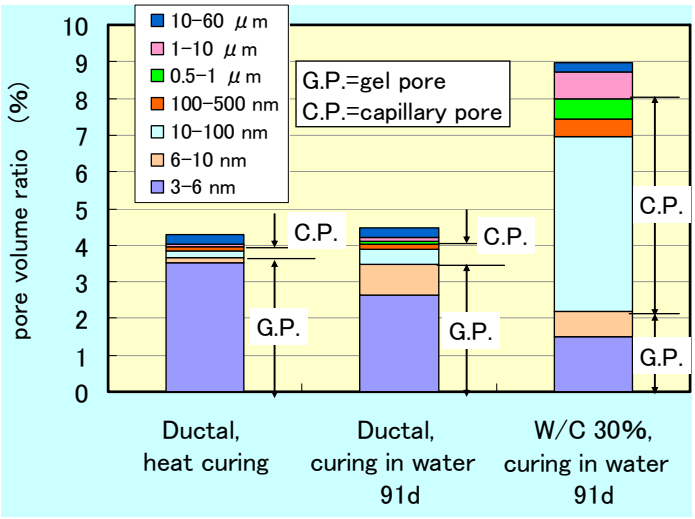

Figure 3. Comparison of pore volume ratio.

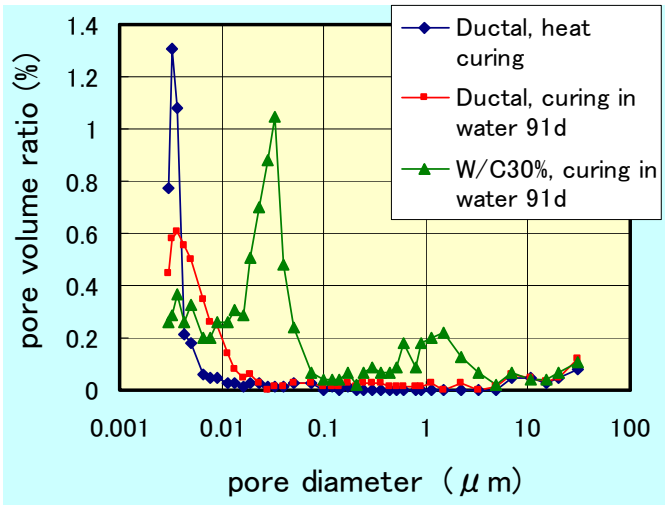

Figure 4. Pore volume ratio distribution.

samples with 90°C heat treatment for 48 hours were cured in the same way as the pre-cast segments. Figure 2 indicates the frequency distribution of compressive strength showing the mean value is 196 N/mm^2 and the standard deviation is 7.1 N/mm^2 for the data number N=48. On the other hand, the results of flexural strength was that the mean value is 36.5 N/mm^2 and the standard deviation is 4.5 N/mm^2 for the data number N=24.

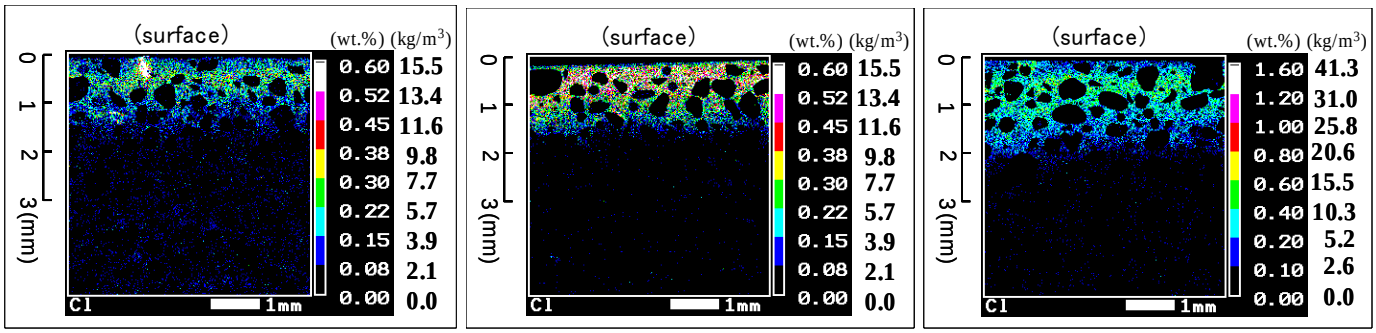

Figure 6. Chloride ions concentration distribution for different immersed periods measured by Electron Probe Micro Analyzer.

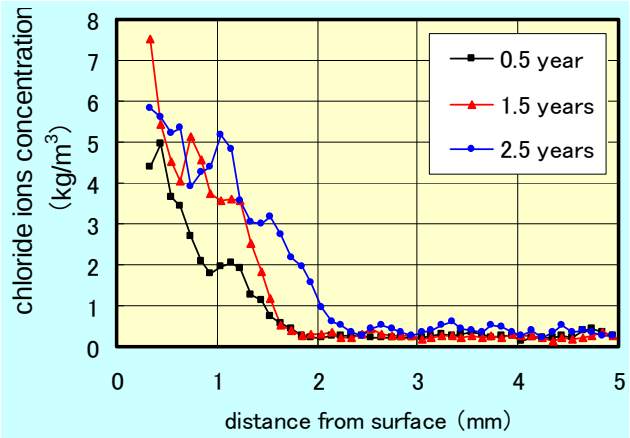

Figure 5. Chloride profiles after different periods.

The incorporation of small-size steel fibers results in ultra-high energy absorption capabilities. The bending fracture energy is 36,000 Nm/m^2, on the other hand one for the ordinary concrete with compressive strength 30~50N/mm^2 is at most a range of 50~200Nm/m^2. The high-tensile strength combined with the high ductility makes conventional reinforcement unnecessary.

The matrix of Ductal® forms a dense structure due to the densest packing and microstructures resulting from pozzolanic reaction of silica fume. The pore size distribution of Ductal® is therefore quite different from the ordinary concrete. Figures 3-4 show the comparison of pore size distribution between Ductal® and the ordinary high strength concrete with W/C=30%. The relationship between the pore volume ratio and the pore diameter was predicted by applying a mercury intrusion porosimetry apparatus. The pore structure is designated depending on the pore size; i.e. it is defined as 'Gel Pore' for the size up to 10nm on the other hand it is defined as 'Capillary Pore' for the size from 10nm to 1μm. The capillary pore is a continuous pore like ameba and this is related to the water permeability; i.e. the lesser the capillary pore the better durability. It is obvious that Ductal® is extremely denser structure than the ordinary concrete, as Figure 3 showing that the pore volume ratio of Ductal® for either heat curing or curing in water are 4.3-4.5%, hence that for high strength concrete with W/C=30% is 9.0%.

Table 2. Apparent chloride ion diffusion coefficient.

immersed priods (year)	0.5	1.5	2.5
apparent chloride diffusion coeff. (cm^2/year)	0.0059	0.0022	0.0019

In addition, the pore volume ratio of capillary pore of Ductal® is only 0.5%, hence that for high concrete is 5.8%.

Carrying out 1100 freezing and thawing cycles in accordance with JIS A 6204 produces no adverse effect on the specimens; i.e. no relative dynamic elastic modulus reductions for 1100 cycles. The extreme denseness of Ductal® makes it difficult to determine the diffusion coefficient of chloride ions. For the estimation of chloride diffusion coefficient, the specimen with 10x10x40 cm was immersed in a NaCl solution (1.9% consistency) for couple of years and EPMA (Electron Probe Micro Analyzer) was used to predict the apparent chloride diffusion coefficient through the regression curves to fit the chloride concentration distribution near the specimen surface. Figure 5 demonstrates the chloride ions concentration profiles after different immersed periods. The pixel size was 0.02 mm and every five-pixel data were averaged in depth direction; i.e. the interval of averaged data in Figure 5 is 0.1 mm. The chloride concentration distribution measured by EPMA for different immersed periods is illustrated in Figure 6. The regression curves to fit the chloride ions concentration designate the apparent chloride diffusion coefficient for those different immersed periods. The chloride diffusion coefficients determined by this method are shown in Table 2. Those results imply the apparent diffusion coefficient ranging from 0.0019 to 0.0059cm^2/year. For comparison, the value for conventional high strength concrete with W/C=30%, which is regarded as having relatively high durability, is 0.14 cm^2/year. The durability properties of Ductal® therefore show a striking difference from those of the conventional normal concrete.

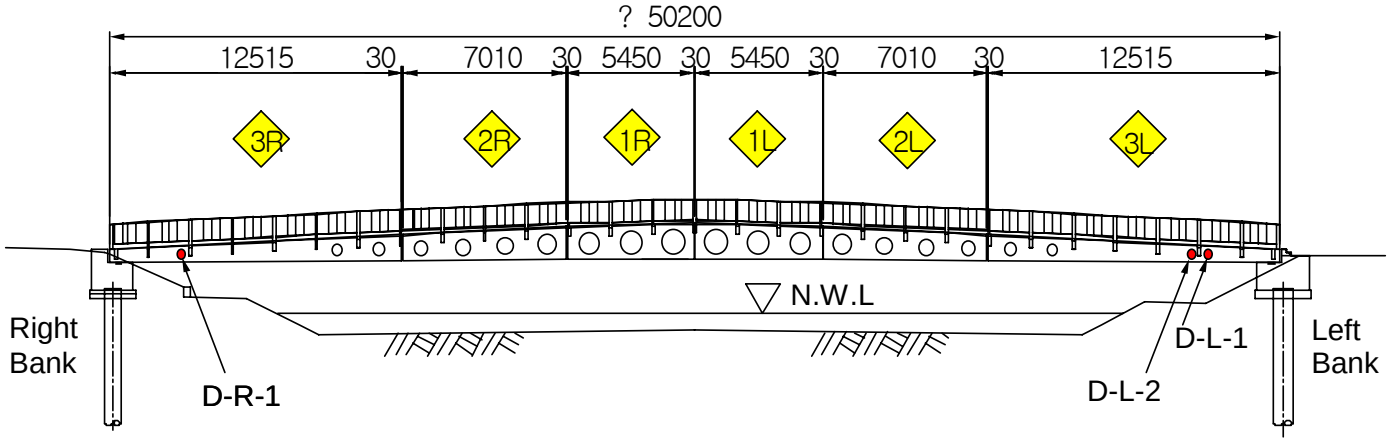

Figure 7. Pre-cast segments composition and aesthetic observation points of downstream side.

Photograph 2. Section of 1R pre-cast segment.

Photograph 3. Installation of 3L pre-cst segment.

2.3 *Design concept of footbridge*

Sakata-Mirai Footbridge was planed to replace four spans old pre-stressed concrete pedestrian bridge that was built about 45 years ago crossing over the Niita River located in Sakata City. Therefore, the following restrictions were requested to make design and to construct the new bridge; i.e. 1) the ground level or the ground slope should not be changed, 2) the bridge bottom line should not be less than 0.6 m from the high water level and 3) the longitudinal slope of the bridge should be less than 5%. From the point of view of river management and the prevention of boats from crush accidents, old piers for bridge were requested to move and one long span bridge is chosen to design. Because of the three restrictions described above, the bridge height at both ends should be less than 55cm.

In order to take the full advantage of the characteristics of UFC and especially to use it without any passive reinforcement, the structural concept and unique points of Sakata-Mirai Footbridge are as follows; i.e. 1) all pre-stressing cables were set outside of the cross section with deviators, 2) ultimate thin slab (5cm) and web (8cm) were employed to reduce the self dead weight, 3) the perforated webs were employed for the sake of design view and reduction

Photograph 4. Exposed specimens inside girder.

of dead weight, 4) eight pre-cast segments were transversely and longitudinally connected to each other by wet joint and 5) no passive reinforcement by rebars even for the pre-stressing anchorage.

The pre-cast segments are composed of two types of segments as shown in Figure 7; i.e. one is closed-form cross-section defined by 1L, 2L, 1R and 2R. Another one is defined by 3L or 3R that are composed of two symmetrical segments being divided into half at the center of the cross section. The total dead weight resulted in 560kN and the total UFC

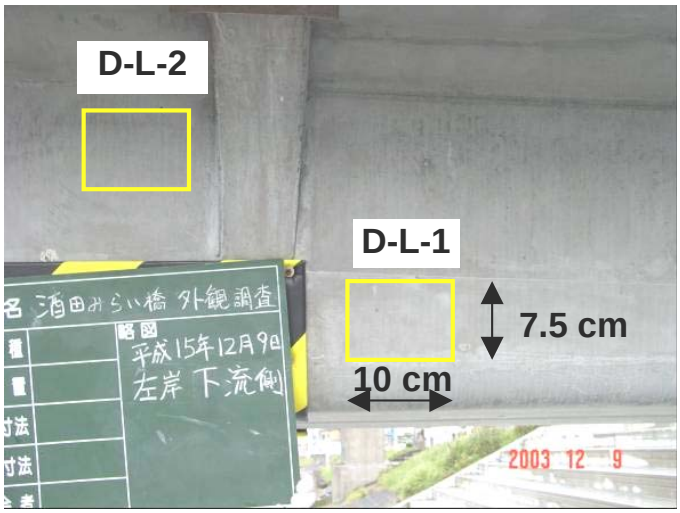

Photograph 5. Aesthetic observation masking of D-L-2 and D-L-2 on downstream side.

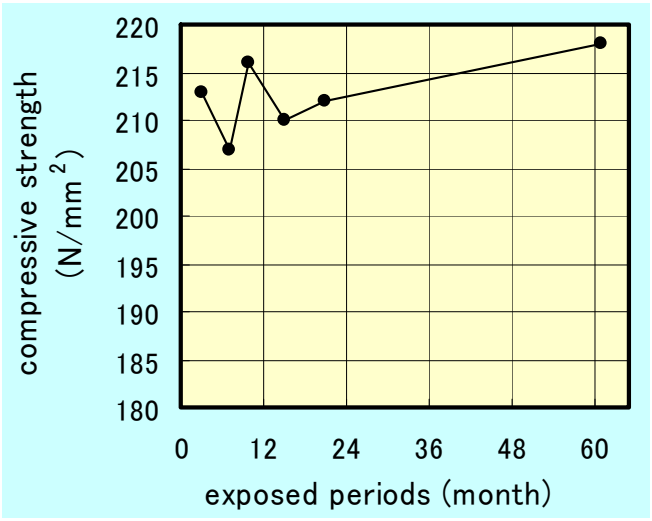

Figure 8. Time history records of compressive strength.

volume became 22m^3 due to the technical design efforts and material advantages. If ordinary pre-stressed concrete were applied for this bridge, then the total dead weight would become 2780kN.

2.4 *Fabrication and installation of segments*

The closed form pre-cast segment as shown in Photograph 2 has some circular holes in the web. This segment was fabricated by casting UFC at once. Therefore the inner mold for this segment is fixed with the outer mold by bolts through the circular holes. After preliminary curing was performed for 48 hours at 30^{o}C, the segment specimen was released from the mold and it was then subjected to 48 hours heat treatment at 90^{o}C. Photograph 3 demonstrates the installation of 3L segment that has already been connected laterally by two symmetrical segments and been pre-stressed by 1S12.7 mono-strand, that supplies about 100kN/tendon pre-stressed force. The dead weight of pre-cast segments was ranged from 57 to 135kN, therefore 1,600kN capacity truck crane was used to install six segments with 30 mm gap and it

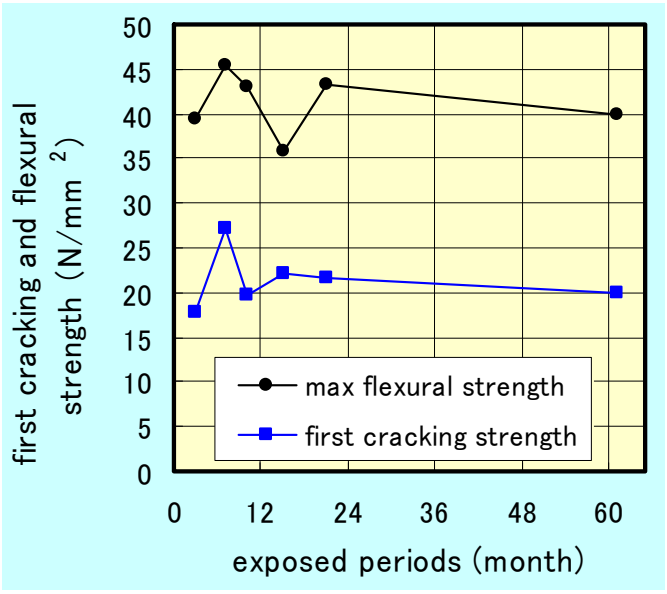

Figure 9. Time history records of flexural strength.

took one day to install all segments. After UHPFRC for wet joint being cured by heat treatment due to electric heater, the longitudinal pre-stressing was carried out by two sets of 31S15.2 tendon

3 FIELD OBSERVAION

3.1 *Secular distortion of mechanical properties*

In order to investigate the material time history of mechanical properties and durability, UFC specimens were exposed inside of the box girder of the footbridge as shown in Photograph 4. The dimension of the specimen for compressive strength is ϕ5x10 cm circular cylinder and that for flexural strength is 4x4x16 cm regular prism. The result of compressive strength versus exposing duration time is shown in Figure 8 and those of flexural strength and first cracking strength are shown in Figure 9. The compressive strength seems to be gradually increasing but it can be said that the strength is stable. It is noted that the average compressive strength in Figure 8 is larger than that in Figure 2. This is because of the size effect on strength; i.e. the size of specimens in Figure 8 is small. The time dependent records of the flexural strength are also stable. The strength of ordinary concrete has usually the upward trend in time, however UFC had heat curing in the process of fabrication; therefore the chemical hydration has already completed. This means the strength would not largely increase.

3.2 *Aesthetic changes due to chloride attack*

The surface aesthetic changes of the footbridge have been investigated. The observation points of inside web surface belong to the pre-cast segments 1L, 1R,

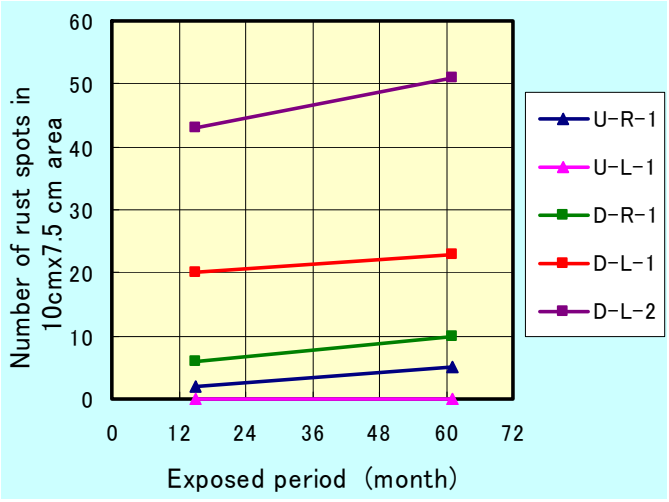

Figure 10. Time history records of rust spots density.

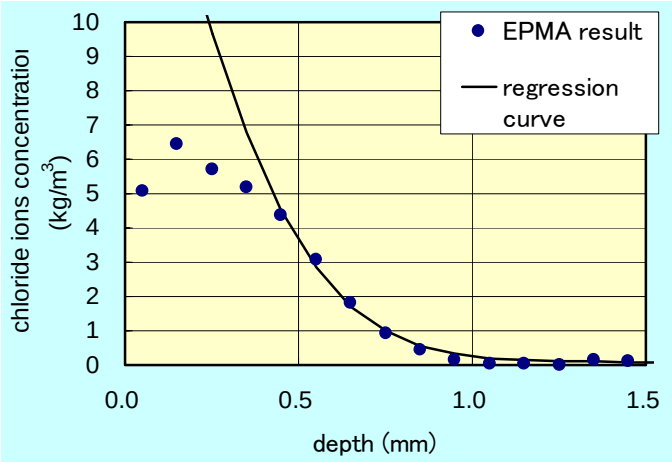

Figure 11. Chloride ions concentration and regression curve.

2L and 2R. On the other hand, those of outside web surface belong to the pre-cast segments 3L and 3R.

The investigation on aesthetic changes (changes of tiny rust spots) were conducted by taking pictures through the masking frame with 10x7.5 cm and counting the rust spots numbers within the masking frame.

The inspection result of aesthetic changes is shown in Figure 10. The aesthetic observation points are illustrated in Figure 7. Rust spots on the surface were not found inside web surface, but found outside web surface. Compared the downstream side web and the upstream side web, it is obvious that the rust spots density on the downstream side web is heavier than the upstream side. The reason is that the downstream side web have been attacked sever corrosive wind and storm in winter. The rust spots density on the downstream side web show tendency to gradually increase, however any deteriorated changes on the matrix could not been seen around the rust spots for 5 years exposed duration time. In addition, the actual aesthetic grade seems to be negligible. Photograph 5 was taken 1 m away from the face of D-L-1 and D-L-2 spot and it is difficult to perceive the rust spots with eyesight. The rust spots seem to be generated when some steel fibers remain near the surface.

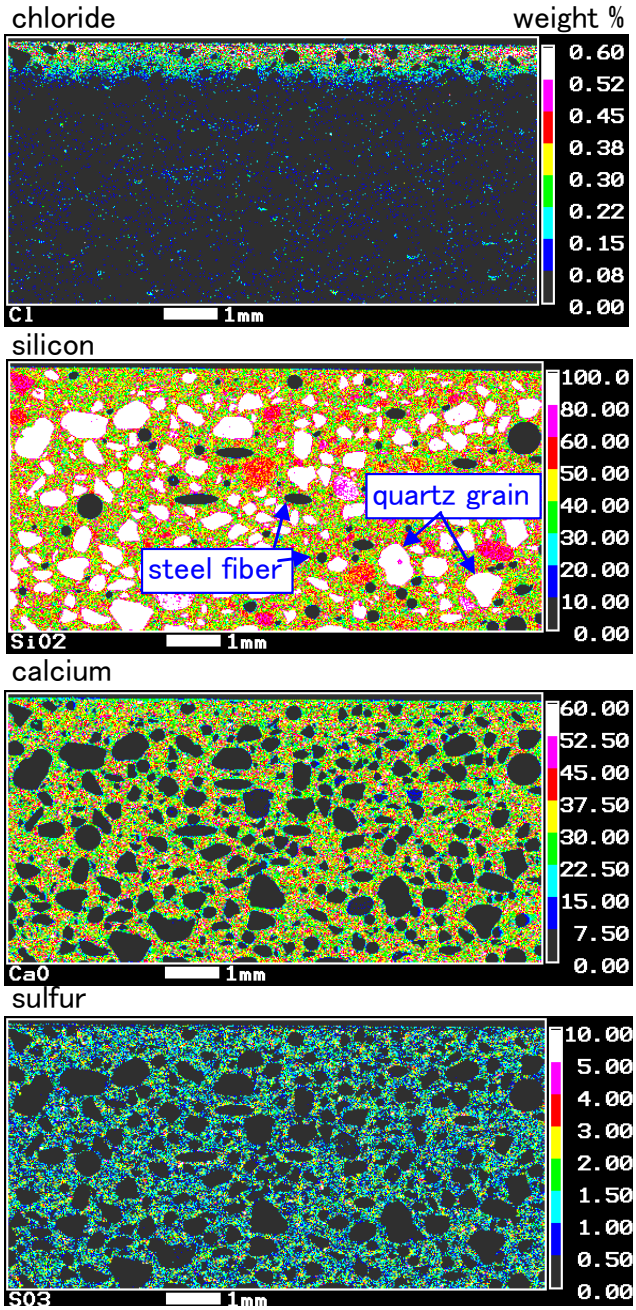

Figure 12. Chloride, Silicon, Calcium and Sulfur concentration profile measured by EPMA.

For example when the matrix cover thickness is zero or 10-20 μm, tiny spot of steel fiber reacts with chloride iron, water and oxygen. However, because matrix around the steel fiber is extremely dense and hard to intrude chloride ions, corrosion would not progress further more.

3.3 *Chloride ions concentration profiles*

The specimen with 4x4x16 cm regular prism that was exposed for 61 months (about 5 years) inside the box shaped girder, was sliced off 10 mm thickness. The dimension of the test surface was taken to be 10 mm in width and 5 mm in depth from the surface and this piece was grinded to apply EPMA. The chloride ions concentration profile and the regression curve are illustrated in Figure 11. The pixel size

was 0.02 mm and every 5 pixel data were averaged in depth direction. The regression data was taken at deeper points of 0.4 mm. It should be noted that compared to the test specimen that was immersed in a NaCl solution (shown in Fig. 5), this concentration profile of the chloride ions is smooth and fits the regression curve quite well. From the regression function, the apparent chloride ion diffusion coefficient was predicted to be 0.000148 cm^2/year that is very small compared to the immersed case and the chloride ion concentration on the surface was calculated to be 18.9 kg/m^3.

Figure 12 indicates the chloride, silicon, calcium and sulfur distribution obtained by EPMA. When compared those four pictures, not only the chloride intrusion but also the steel fiber, quartz grain, and hydrate substance can be identified. For example, from the result of silicon picture, small black dots must be steel fiber, large circular black dots must be entrapped air, white polygon must be quartz grain and rest of yellowish green must hydrate substance. It should be noted that corrosive environment of this footbridge may be much severe than what we considered in design stage from the information that the chloride ion concentration on the surface was derived to be 18.9 kg/m^3.

4 CONCLUSIONS

1) The time dependent records of compressive and flexural strength were stable.
2) Aesthetic changes on the UFC surface could not be observed except the downstream outside web where chloride ions may be concentrated.
3) Rust spots were actually hard to find out with eyesight and no deteriorated changes on the matrix could be observed around the rust spots.
4) Chloride ion diffusion coefficient obtained the field specimen was much lower than that in the laboratory immersed specimen.

PREFERENCES

JSCE 2004. Recommendation for Design and Construction Ultra High Strength Fiber Reinforced Concrete Structures-Draft. *Concrete Library No 113.*

Tanaka, Y. & Musha, H. & Ootake, A. & Shimoyama, Y. & Kaneko, O. 2002. Design and Construction of Sakata Mirai Footbridge using Reactive Powder Concrete, *Proc. of 1st fib Congress 2002, Oosaka.*